GEOSTATISTICAL ANALYSIS FOR SPATIAL EVALUATION OF LIQUEFACTION POTENTIAL IN SAITAMA CITY

Rama Mohan Pokhrel [1]*, Jiro Kuwano [2] and Shinya Tachibana [3]

ABSTRACT: The liquefaction potential (P_L) values within the sedimentary basins are variable within short distances. If P_L value does not exist quantitatively at a location of interest then data collected at other locations must be used to estimate the value for the desired locations. The aim of this study is the application of geostatistical method using randomly distributed measured liquefaction potential data to estimate more reliable P_L value where measured data is not available. An experimental semivariogram was constructed from these randomly distributed measured locations to characterize the spatial variability of the measured P_L value. A model semivariogram curve for isotropic and anisotropic modeling was fitted for the experimental curve to estimate the P_L value for the unsampled locations. Using these model curves the potential value for the unsampled locations was estimated. To check the validity of the method and better model the estimated P_L value was correlated with the measured P_L value at the same locations. The greater R^2 value given by the anisotropic model shows the benifit of anisotropic modeling in liquefaction potential mapping.

Keywords: Liquefaction potential, GIS, geostatistical method, zoning, Saitama city.

INTRODUCTION

Soil liquefaction is an earthquake ground failure mechanism that occurs in loose, saturated granular sediments particularly sand and silty sand. It was a major cause of damage to soil structures, lifeline facilities and building foundations in past earthquakes and clearly poses a significant threat to the integrity of structures and facilities during future earthquakes. Some of the examples from past earthquakes have proved that the local site condition plays an important role for the spatial variation of liquefaction potential because the damage caused by the earthquake is different even in very near places. Therefore spatial variation of liquefaction potential should be zoned by using proper methodology. Liquefaction potential zoning is the process of identification of an area having different liquefaction hazard potentials. The main purpose of liquefaction potential zoning is to prepare a map to identify the significant possibility of severe disaster and ground disturbances during seismic events.

In the conventional approach borehole data are used to evaluate the liquefaction potential at any point. But it is not always possible to measure the liquefaction potential of the borehole point at every location. Therefore, it is essential to evaluate the liquefaction potential in the area where borehole data is not available. The traditional approach to evaluate liquefaction potential at such area is correlation with geology and geomorphology which is not always reliable. Therefore, in this study, a kriging method in geostatistical analysis in Geographic Information System (GIS) platform is introduced to evaluate the liquefaction potential at unsampled locations. Interpolation methods such as IDW, moving average, triangulation etc are affected by distribution and numbers of data locations usually in the case of not uniform in the study area. However kriging method can evaluate spatial distribution of a certain value by unbiased interpolation even if sampled data are not distributed uniformly.

The kriging method of interpolation in geostatistical analyst was used in different fields such as precipitation, elevation, air temperature, evapotranspiration, soil properties, ground water level, electrical conductivities, soil contamination (Kumar and Remadevi 2006), (Gundogdu and Guney 2007), (Nikroo et al. 2010). Kriging method is used in the geotechnical field by various researchers. Maruyama et al. (2010) used simple

---

[1] Geosphere Research Institute (GRIS), Department of Civil and Environmental Engineering, Saitama University, Saitama, Japan, *corresponding author, E-mail: pokhrel_rmohan@yahoo.com
[2] Professor, Geosphere Research Institute (GRIS), Department of Civil and Environmental Engineering, Saitama University, Saitama, Japan, E-mail: jkuwano@mail.saitama-u.ac.jp
[3] Assistant Professor, Geosphere Research Institute (GRIS), Department of Civil and Environmental Engineering, Saitama University, Saitama, Japan, E-mail: stachi@mail.saitama-u.ac.jp
Note: Discussion on this paper is open until December 2012

kriging method to estimate peak ground velocities for the investigation of relationship between PGVs and damage ratio of the expressway. Thompson et al. (2010) used kriging method to mapping site response spectral amplifications. Kriging interpolation method was used for liquefaction potential estimation at unsampled locations where the data are not available (Baise et al. 2006), (Chen et al. 2008), (Pokhrel et al. 2010), (Chung et al. 2011) but there are lacks of validation of results.

In kriging method, the first step is to examine the data to identify the spatial structure, which often represented by the empirical variogram (Isaaks and Srivastava 1989). The data in the empirical variogram are fitted with the proposed variogram function to model spatial autocorrelation. In practice, the success of kriging maps is dependent on the suitability of the modeled semivariogram to the data at hand (Sen and Sahin 2001). The weighted values are derived from this semivariogram function. The linear or non-linear combinations of these weights and the corresponding observed values are used to estimate values at unsampled locations (George and Wong 2008). The main advantage of this approach is that the spatial characteristics are taken into account.

STUDY AREA

Saitama city is the capital and most populated city of Saitama prefecture in Japan. It is situated in the south east of the prefecture and located 20 to 30 km north of central Tokyo Fig. 1. The city is topographically comprised of lowlands and plateaus mostly fall below 20 m above the sea level Fig.1 at the middle part of Kanto plain of Japan. The Arakawa River flows from northwest to southeast along the western boundary of the study area. Therefore the western portion of the city lies on the lowland (flood plain) created by the Arakawa River. The Ayase and Motoarakawa rivers are also flows northwest to southeast from the eastern part of the area.

There were uncountable numbers of small earthquakes in the study area. But all these earthquakes are not hazardous for the city. Some of the earthquakes which were hazardous and caused severe liquefaction on the study area were summarized in the Table 1. The locations of these liquefaction areas are plotted on the location map in Fig. 1 The first known liquefaction record in the Saitama area was caused due to 1703 Genroku Earthquake of magnitude 7.9 to 8.2 (Wakamatsu 1992). Among these liquefaction histories the western portion flood plain of the Arakwa River and the eastern portion which is
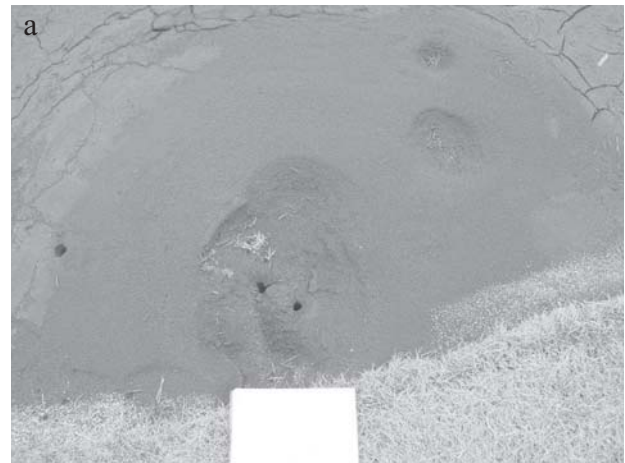
Fig. 2 Liquefaction observed in the golf course at study area along the Arakawa River due to the Tohoku earthquake Japan on 11th March 2011 (a) sand volcano and (b) fracture on the ground the location of photographs are shown P on the map fig. 1.
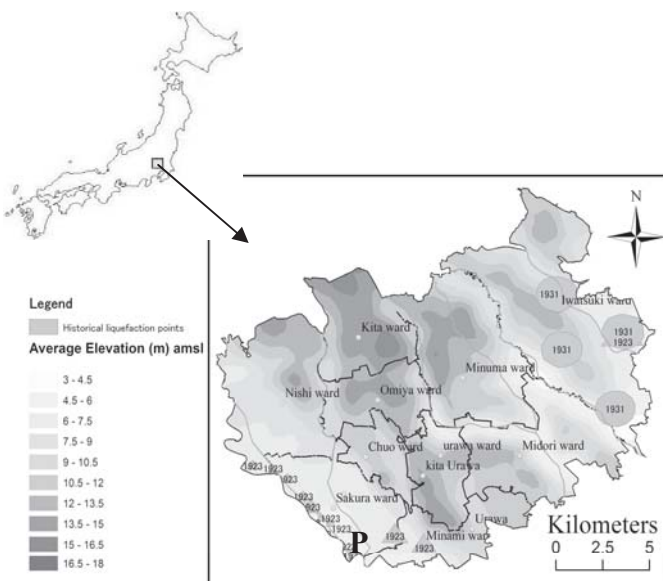
Fig. 1 Location map of the study area with topography and historical liquefaction points

Table 1 Earthquakes which caused liquefaction in Saitama (Wakamatsu 1992)

Date	Name of earthquake	Magnitude (JMA)	Affected Area
1703.12.31	Genroku Earthquake	7.9~8.2	Edo, Kanto Region
1855.11.11	Edo Earthquake	6.9±0.1	Edo and surrounding area
1891.10.28	Nobi Earthquake	8.0	Aichi and Gifu area
1894.6.20	North Tokyo Bay	7.0	North Tokyo Bay
1895.1.18	Kasumigaura	7.2	Kasumigaura, Ibaraki
1923.9.1	Great Kanto Earthquake	7.9	South Kanto Region
1931.9.21	Nishi Saitama Earthquake	6.9	Central Saitama Region

situated on the recent alluvial sediments liquefied more. However, there is no record of liquefaction in the history at the middle part of the study area which lies on the Omiya plateau several locations in the study area liquefied at the time of the Great Kanto earthquake of magnitude 7.9. The liquefaction in the study area Fig.2 was observed in the Tohoku earthquake of magnitude 9.0 on 11th March 2011. In this figure shows the sand volcano and fracture on the ground due to liquefaction in the study area.

METHODOLOGY

Kriging is a geostatistical technique of interpolation that considers both the distance and the degree of variation among known data points when estimating values in unknown areas. In the kriging the first step is to examine the data to identify the spatial structure, which often represented by the empirical semivariogram (Isaaks and Srivastava 1989). A semivariogram is a figure showing the relationship between semivariance
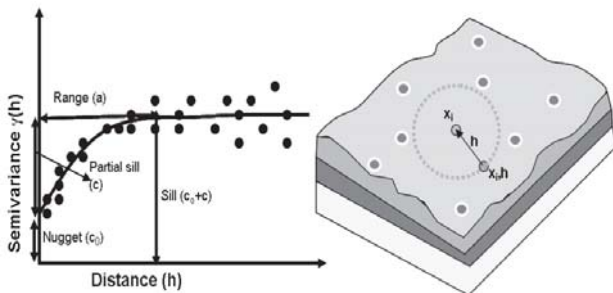

Fig. 3 Ordinary Kriging variogram model

and the distance between all the pair of available data locations as schematically illustrated in Fig.3.

The experimental semivariance for liquefaction potential is calculated by using the following Equation (1):

$$\gamma(h) = \frac{1}{2N(h)} \sum_{i=1}^{N(h)} \left(P_L(i) - P_L(i,h) \right)^2 \tag{1}$$

Where $\gamma(h)$ is estimated value of the semivariance for a distance h; $N(h)$ is the number of paired data at the distance of h; $P_L(i) - P_L(i, h)$ is a difference in P_L of ith paired locations whose distance is h.

The experimental variogram was made for the liquefaction potential values evaluated at each sampled borehole data. It gives the degree of relationship between points on the surface. This empirical variogram was fitted to the theoretical variogram function to model spatial autocorrelation curve as shown in Fig. 3. For this study a spherical model shown in Equation (2) is fitted by using weighted least square error method.

$$\gamma(h) = c_0 + c\left[\frac{3h}{2a} - \frac{h^3}{2a^3} \right] \text{ for } 0 < h \leq a \tag{2}$$

where c_0 is a nugget, a is a range, c is a partial sill, c_0+c is total sill, h is a lag distance and $\gamma(h)$ is semivariance value. It quantifies a basic principle of things which closer are more alike than things farther apart.

In kriging once the model variogram is constructed, it is used to compute the weights. This weight is used to evaluate the liquefaction potential at any point in the study area with the Equation (3).

$$p_L(x,y) = \sum_{i=1}^{n} \lambda_i(x_i, y_i) p_L(i) \tag{3}$$

Where $P_L(x,y)$ is P_L at (x,y) estimated by interpolation; $P_L(i)$ is the evaluated P_L value at the ith location; $\lambda_i(x_i,y_i)$ weight for $P_L(i)$ to estimate $P_L(x,y)$; n is a number of locations used for the kriging interpolation. In kriging, weights are based not only on the distance between the measured points and the prediction location but also on the overall spatial relationships among the measured values around the prediction location, that is model variogram as shown in Fig. 3.

The consideration in the above assumes that the spatial correlation structure is same in all directions or isotropic. In this case the semivariogram model depends only on the magnitude of the distance not in the direction. However, it is quite natural for the behavior of a data set to vary differently in one direction as compared to another which is known as anisotropy as illustrated in

Fig.4. To check directional anisotropy in an experimental semivariogram, semivariance values are calculated for data pairs falling within certain directional
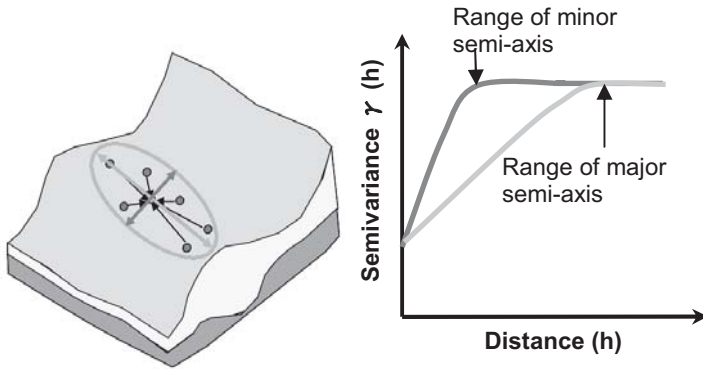

Fig. 4 Schematic diagram of anisotropic model for the liquefaction potential

bands. The directional bands are specified by a given angle in a certain direction, with certain angle of tolerance. To consider the anisotropy in analysis, it is essential to guiding the kriging interpolation to use sample data points that will most accurately reflect the behavior of the ground conditions. The influence of anisotropy will affect the points of the semivariogram and the model that will be fit. In semivariogram the model curve of the anisotropy shows the longer range in major semi-axis direction and short range in minor semi-axis direction as illustrated in Fig.4.

In this study, the result of the kriging interpolation made for the first set of data is compared with the second set of data which are also randomly distributed throughout the study area. There are 41 borehole locations in the second set of data. The predicted values at the second set of data locations were plotted against the values directly evaluated from the second set of data values and the regression coefficient was calculated.

RESULTS

Fig. 5 is a liquefaction potential map obtained after plotting estimated liquefaction potential at 86 sampled boreholes. The liquefaction potential ranging from 0 to 100 is classified in three groups as $0<P_L<5$ as low, $5<P_L<15$ as high and $15<P_L$ as very high liquefaction potential (Iwasaski et al. 1978). In this paper the liquefaction potential area is classified on the basis of P_L value. The severity of damage increases with the increase of P_L value.

A semivariogram was prepared for the inspection of the PL values measured at the sampled boreholes. Fig. 6 shows the empirical and modeled semivariogram curve of PL. The ordinary kriging spherical model is relevant

for these data where the nugget of this curve is 96.3, the partial sill is 170 and range is 1.85km.
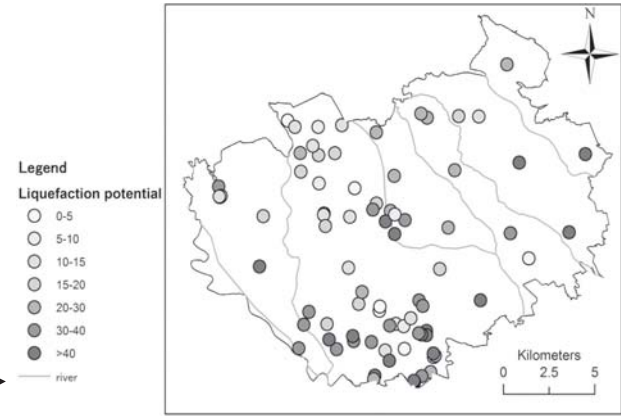

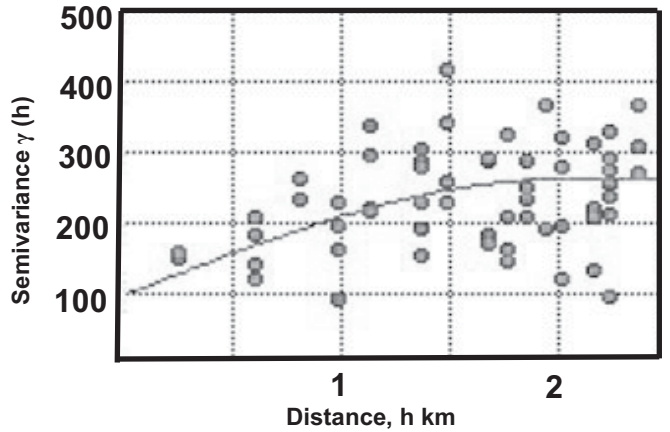Fig. 5 Liquefaction potential at the first set of borehole locations

Fig 6 Ordinary Kriging Empirical (dots) and fitted model (curve line) semivariogram for P_L value

The equation of model semivariogram curve is shown in Equation (4).

$$\gamma(h) = 96.3 + 170 \frac{h}{3.7}\left[3 - \frac{h^2}{1.85^2}\right] \qquad (4)$$

Where h is lag distance and $\gamma(h)$ is a semivariance. The nugget to sill ratio is 0.3616 that indicates the moderate spatial dependence of the data.

In the study area the anisotropy appears due to the ancient flow direction of the rivers and topography. Therefore anisotrophic consideration was accounted for the analysis. In this area the major semi-axis of the anisotropy is along N10^{0}W and minor semi-axis is perpendicular direction of the major semi-axis. The range along the major semi-axis is 3.45 km and along minor semi-axis is 1.44 km which are shown in the Fig.7.

In Fig.7 the triangular points have semivariance value plotted for all paired of data in parallel to N10^{0}W to each other and square points are paired of location

with parallel to N80⁰E to each other. Fig. 8 shows the continuous liquefaction potential map of the study area using the application of ordinary kriging method. Fig.8 (a) shows the map considering the isotropic condition of
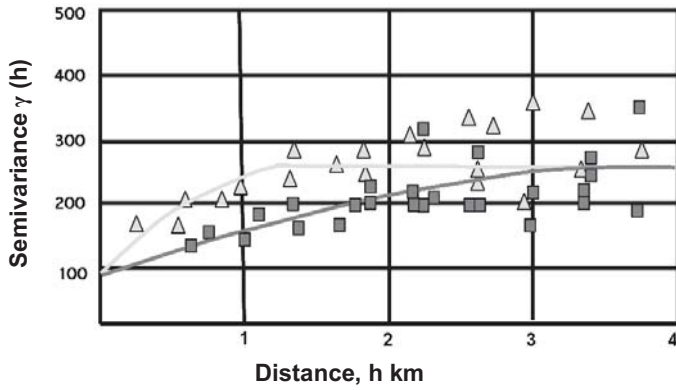

Fig 7 Anisotropic semivariogram model for the study area

the ground and application of isotropic model. Similarly Fig.8 (b) shows the map prepared using anisotropic model analysis. All the historical liquefaction locations indicated in Fig.1of the study area fall on the extremely high (>40) liquefaction potential area in Fig.8.

The map thus prepared is validated with the second set of 41 boring data which are randomly distributed in the study area. The first set and second set of data were
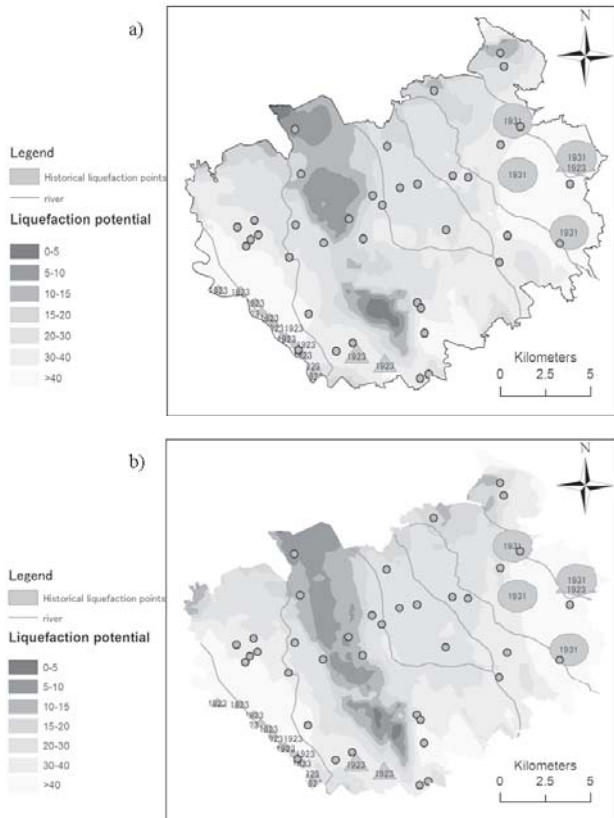

Fig 8 Continuous liquefaction potential map and locations of second set of data on (a) isotropic (b) anisotropic consideration map

collected independently. Fig. 8 shows the location of second set of borehole data (red dots) in the continuous liquefaction potential map prepared from the first set of data. At the location of each borehole of the second set of data, the interpolated data was also obtained from the continuous liquefaction potential map. The liquefaction potentials evaluated at the locations of the second set of boreholes were compared with the interpolated liquefaction potential at the same location of the second set of data as shown in Fig. 9.
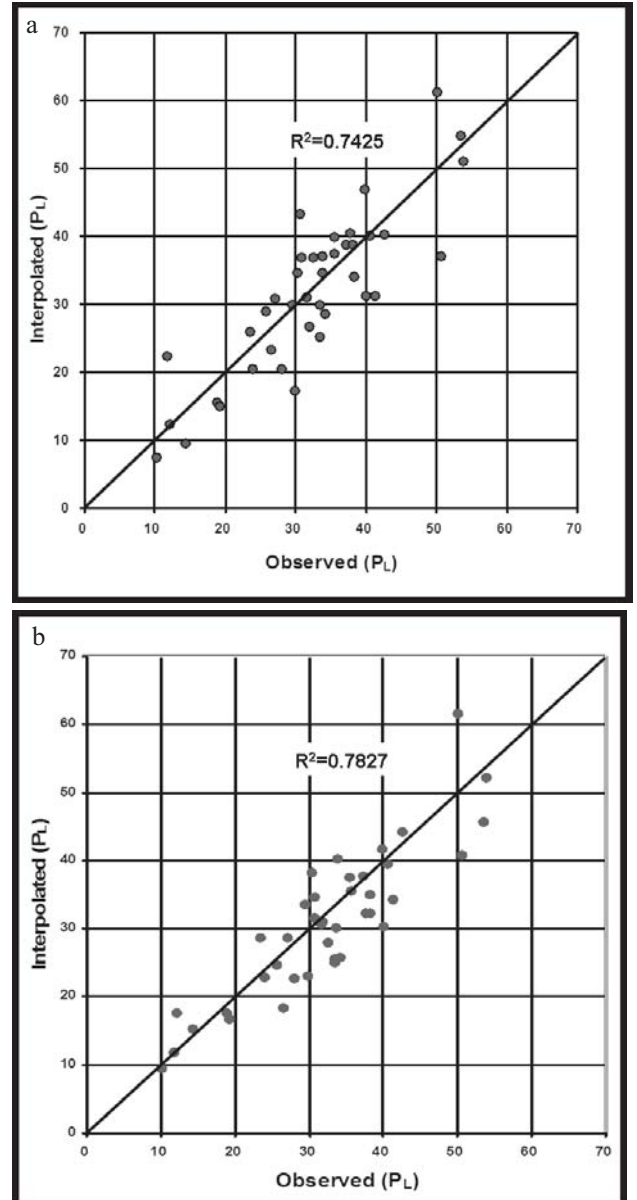

Fig 9 Comparison of directly evaluated and interpolated P_L at the second set of data (a) with isotropic consideration (b) anisotropic analysis

The P_L value evaluated from the first set of data shows good coincidence with P_L obtained from the second set of borehole data. The R^2 value from the anisotropic

consideration is 0.7827 and from the isotropic consideration is 0.7425 (as shown in Fig.9). It indicates that anisotropic consideration gives better result. The historical liquefied points Fig.1 are plotted in the zone of high liquefaction in the liquefaction potential map this result also indicates the suitability of the method.

CONCLUSIONS

Liquefaction potential map is valuable information for seismic hazard and its mitigation in an area. The liquefaction potential value changes with soil properties over short horizontal distances, especially in the recent alluvial deposits. In such area, it is essential to evaluate the liquefaction potential value at every point.

In the present study, 2 sets of independent borehole data are collected and liquefaction potential value was calculated for each boreholes. kriging method of interpolation in geostatistical analysis was used to estimate the liquefaction potential at the unsampled area. First set of data was used to prepare a liquefaction potential map by interpolating. For each borehole location of second set of data the interpolated (P_L) given by first set of boreholes value were collected and compare with measured P_L value. This study shows that kriging method of interpolation is a suitable and unbiased method for the liquefaction potential mapping because the data set shows significance correlation. The R^2 value from the anisotropic analysis is slightly greater than isotropic analysis (0.7827>0.7425) showing that the anisotropic consideration is to be made in to interpolating the value at the unsampled locations. The historical liquefaction points are plotted in the zone of high liquefaction potential also indicates suitability of the method. This study shows that the southern part and the western part along the Arakawa River and eastern part along the Minuma River and Shiba River in Saitama City have extremely high liquefaction potential. The center of the city along Omiya plateau has low liquefaction potential. This method cannot give significance result at ground surface with complex geology like faults.

ACKNOWLEDGEMENTS

REFERENCES

Baise, L.G., ASCE, M., Higgins, R.B. and Brankman, C.M. (2006) "Liquefaction hazard mapping-statistical and spatial characterization of susceptible units" Journal of Geotechnical and Geoenvironmental Engineering, ASCE, pp 705-715.

Chen, G.X., Tang, H. and Kan, S.Z. (2008). Kriging interpolation method and 2.5D GIS applied in the probabilistic estimation of seismic site liquefaction. Proceeding of 12th international conference of international association for computer methods and advances in Geomechanics (IACMAG) Goa, India, pp 2998- 3004.

Chung, J.W., Rogers, J.D. and Masce, P.E. (2011) "Simplified method for spatial evaluation of liquefaction potential in the St. Louis area" Journal of Geotechnical and Geoenvironmental Engineering, ASCE, Vol 137, No.5, pp 505-515.

George, Y.L. and Wong, D.W. (2008) "An adaptive inverse-distance weighting spatial interpolation technique."Computers and Geotechniques, vol. 34 1044-1055.

Gundougdu, K.S. and Guney, I. (2007) "Spatial analyses of groundwater levels using universal kriging" Journal of earth system science 116 No.1 pp.49-55.

Isaaks, E.H. and Srivastava, R.M. (1989). An Introduction to Applied Geostatistics. Oxford University press, Oxford, 561pp.

Iwasaki, T., Tatsuoka, F., Tokida, K. and Yasuda, S. (1978) A practical Method for Assessing Soil Liquefaction Potential Based on Case Studies at Various Sites in Japan, Proc. 2nd International Conference on Microzonation, San Francisco, Vol.2, pp. 885-896.

Kumar,V. and Remadevi (2006). Kriging of Groundwater levels- A case Study. Journal of Spatial Hydrology, Vol.6, No.1

Maruyama, Y., Yamazaki, F., Mizuno, K., Tsuchiya, Y. and Yogai, H. (2010) Fragility curves for expressway embankments based on damage datasets after recent earthquakes in Japan. Soil Dynamics and Earthquake Engineering vol. 30, 1158-1167.

Nikroo, L., Kompani-Zare, M., Sepaskhah, A.R. and Fallah Shamsi, S.R. (2010) "Groundwater depth and elevation interpolation by kriging method in Mohr Basin of Fars province in Iran" Environ Monit Assess 166:387-407.

Pokhrel, R. M., Kuwano, J. and Tachibana, S. (2010). Liquefaction hazard zonation mapping of the Saitama City, Japan. Journal of Nepal Geological Society, Vol. 40, pp. 69-76

Sen, Z. and Sahin, A.D. (2001). Spatial interpolation and estimation of solar irradiation by cumulative Semivariograms. Solar Energy 71 (1), 11-21.

Thompson, E.M., Baise, L.G., Kayen, R.E., Tanaka, Y. and Tanaka, H. (2010). A geostatistical approach to mapping site response spectral amplifications. Engineering Geology 114, 330-342.

Wakamatsu, K. (1992). Maps for Historic Liquefaction Sites in Japan, Published by Tokai University press.